Received: 21 December 2017 | Revised: 11 February 2018 | Accepted: 14 March 2018

DOI: 10.1002/jmr.2719

SPECIAL ISSUE ARTICLE

WILEY Journal of Molecular Recognition

Mechanical and migratory properties of normal, scar, and Dupuytren's fibroblasts

Prem Kumar Viji Babu[1] | Carmela Rianna[1] | Gazanfer Belge[2] | Ursula Mirastschijski[3] | Manfred Radmacher[1]

[1] Institute of Biophysics, University of Bremen, Bremen, Germany

[2] Faculty of Biology and Chemistry, University of Bremen, Bremen, Germany

[3] Department of Plastic, Reconstructive, and Aesthetic Surgery, Klinikum Bremen-Mitte, and Wound Repair Unit, CBIB, University of Bremen, Bremen, Germany

Correspondence
Manfred Radmacher, Institute of Biophysics, University of Bremen, Bremen, Germany.
Email: mr@biophysik.uni-bremen.de

Funding information
Universität Bremen

Abstract

Mechanical properties of myofibroblasts play a key role in Dupuytren's disease. Here, we used atomic force microscopy to measure the viscoelastic properties of 3 different types of human primary fibroblasts derived from a same patient: normal and scar dermal fibroblasts and palmar fascial fibroblasts from Dupuytren's nodules. Different stiffness hydrogels (soft ~1 kPa and stiff ~ 50 kPa) were used as cell culture matrix to mimic the mechanical properties of the natural tissues, and atomic force microscopy step response force curves were used to discriminate between elastic and viscous properties of cells. Since transforming growth factor-β1 (TGF-β1) is known to induce expression of α–smooth muscle actin positive stress fibers in myofibroblasts, we investigated the behavior of these fibroblasts before and after applying TGF-β1. Finally, we performed an *in vitro* cell motility test, the wound healing or scratch assay, to evaluate the migratory properties of these fibroblasts. We found that (1) Dupuytren's fibroblasts are stiffer than normal and scar fibroblasts, the elastic modulus E ranging from 4.4, 2.1, to 1.8 kPa, for Dupuytren's, normal and scar fibroblasts, respectively; (2) TGF-β1 enhances the level of α–smooth muscle actin expression and thus cell stiffness in Dupuytren's fibroblasts (E, ~6.2 kPa); (3) matrix stiffness influences cell mechanical properties most prominently in Dupuytren's fibroblasts; and (4) Dupuytren's fibroblasts migrate slower than the other fibroblasts by a factor of 3. Taking together, our results showed that mechanical and migratory properties of fibroblasts might help to discriminate between different pathological conditions, helping to identify and recognize specific cell phenotypes.

KEYWORDS

AFM, Dupuytren's disease, elastic and viscous properties, myofibroblast, wound healing assay

1 | INTRODUCTION

Dupuytren's disease is a fibromatosis of the connective tissue of the palm that can lead in certain cases to the immobility of one or more fingers due to formation of nodules and cords in the palmar fascia.[1,2]

Connective tissue represents the architectural and supportive framework of many tissue and organs in animal body, and it is mainly composed by fibroblasts. In the palmar fascia of patients with Dupuytren's disease, there is an increase of the type III collagen to type I collagen ratio in the extracellular matrix (ECM)[3] and an increase of the myofibroblast population in the Dupuytren's nodule.[4]

Fibroblasts constitute the predominant cell type in connective tissues. They secrete and deposit ECM components to establish a scaffold for neighboring cells. In wound healing, fibroblast migration and

This article is published in Journal of Molecular Recognition as part of the virtual Special Issue 'AFM BioMed Krakow 2017, edited by Malgorzata Lekka, IFJ PAN, and Pierre Parot , CEA, France, and Jean-Luc Pellequer, IBS, France'

their transdifferentiation into α–smooth muscle actin (α-SMA) expressing myofibroblasts results in the exertion of mechanical stress on the ECM and thus contributes to tissue remodeling.[5] The transition from fibroblasts into myofibroblasts depends on the activation of the latent transforming growth factor-β1 (TGF-β1) that is deposited in the ECM via binding to decorin and the TGF-β latency-associated complex.[6,7] TGF-β1 is a multifunctional protein that increases the expression of α-SMA[8] in concert with the fibronectin ectodomain-A,[9] and α-SMA enhances the contractile activity of myofibroblast. The increased contractility of myofibroblasts leads to stiffening of the ECM. In addition, during the process of wound healing, migrating fibroblasts create mechanical stress on the ECM matrix by adopting a myofibroblast phenotype to generate stress fiber formation and secretion of additional ECM molecule (collagen).[10]

Numerous studies support the idea that myofibroblasts are a key cell responsible for the tissue contraction in Dupuytren's disease. In vitro models have been developed to study the underlying cellular basis of myofibroblast differentiation and contraction. Several studies suggest that the growth factor TGF-β1 combined with mechanical stress can promote the differentiation of fibroblasts into myofibroblasts.[8,11] However, there are no studies reporting the comparison of mechanical properties of fibroblasts extracted from different sites of the same patient affected by Dupuytren's disease.

Atomic force microscopy (AFM) can be used to study cell stiffness,[12,13] cell-cell interaction,[14-16] and cell-ECM interactions.[17,18] Measuring cell stiffness by microindentation using AFM yields information about many biological processes, like migration,[19] cytoskeletal structure,[20] myosin activity, and pathological conditions, in which the alteration in cell mechanical properties allows the discrimination between normal and diseased cells.[21-25]

Here, by using AFM, we measured the viscoelastic properties of 3 types of fibroblasts: normal, scar, and Dupuytren's fibroblasts, extracted from the same patient. Specifically, using AFM step response force curves and analyzing the data using the standard linear solid model, we could compare viscous and elastic properties of the cells. In this experimental scheme, after the step, the force (being proportional to the deflection) and the sample indentation (calculated as z height minus deflection) will relax to a new equilibrium situation. Thus, our experimental scheme is neither equivalent to a strain relaxation experiment, where stress is kept constant, nor a stress relaxation experiment, where strain is kept constant. Technically, we could apply a step in force, which would require an additional feedback to use, which will reduce the time resolution of our setup.[26] Moreover, we studied the effect of TGF-β1 on the mechanical properties of the 3 fibroblasts, as well as on their cytoskeleton organization acquiring fluorescent images of cells where α-SMA has been stained. Since viscoelastic properties of cells strongly depend on substrate stiffness,[27] we used polyacrylamide (PA) gel with different stiffness values as cell culture supports, namely, soft (~1 kPa) and stiff (~50 kPa) gels to further investigate the response of cells to different mechanical signals. Finally, to gain insights in the migratory properties of these fibroblasts and to emulate the conditions of wound healing, we performed a migratory test, so-called wound healing or scratch assay. We could find differences in mechanical properties of the different fibroblasts. Specifically, Dupuytren's fibroblasts were stiffer than the others, and their mechanical properties and cytoskeleton organization were mainly influenced from TGF-β1, as well as from different stiffness of underlying materials. Concerning motility features, α-SMA expressing Dupuytren's myofibroblasts was slower than the other fibroblasts investigated in this study.

2 | MATERIALS AND METHODS

2.1 | General materials

Acrylamide and bisacrylamide solutions were purchased from Bio-Rad. N,N,N′,N′-tetramethylenediamine (TEMED), N-[3-(trimethoxysilyl) propyl]ethylenediamine silane, and dichlorodimethylsilane solutions were purchased from Sigma. Anti-alpha-actin (smooth muscle) rabbit monoclonal antibody, sodium hydroxide, Dulbecco modified Eagle's medium (DMEM), and ammonium persulphate (APS) were purchased from Merck, TGF-β1 from Peprotech, and Alexa Fluor 488 secondary antibody from Life Technologies. Glutaraldehyde, ethanol, and other solvents were purchased from Panreac AppliChem.

2.2 | Gel substrate preparation

Polyacrylamide gels were prepared following a well-established protocol[28] based on the polymerization of the gel solution between 2 glass slides, silanized with aminosilane or chlorosilane, respectively. For the aminosilanization process, round cover slips were first washed with absolute ethanol and ultrapure water (MilliQ systems, Molsheim, France), then covered with 0.1M NaOH for 3 minutes, and finally activated with N-[3-(Trimethoxysilyl)propyl]ethylenediamine silane for 3 minutes and treated with 0.5% glutaraldehyde for 30 minutes. For the chlorosilanized glass preparation, a dichloromethylsilane solution was poured on the cover slides for 5 minutes; glasses were later extensively washed with ultrapure water and dried with paper tissues. Polyacrylamide gel solution was prepared by mixing 40% acrylamide with 2% bisacrylamide in ultrapure water. Polymerization was initiated by APS and TEMED. The gel solution was then poured on the aminosilanized glass and covered with the chlorosilanized one to avoid the presence of oxygen that would inhibit the polymerization. After 30 minutes, the upper slide was removed while the gels were attached on the aminosilanized supports. By varying the amount of bisacrylamide, we obtained gels with different stiffness values. Here, we made soft and stiff gels with elastic moduli of ~1 kPa and ~50 kPa, respectively (values were measured by using AFM), to study the mechanics of fibroblasts from 3 different origins. Before cell seeding on PA gel, the substrates were sterilized in ethanol, extensively washed in PBS, and incubated with DMEM medium along with 20% fetal bovine serum for a few hours to promote serum protein adsorption on the gels.

2.3 | Cell isolation and cell culture

Primary fibroblasts were isolated from 3 surgically removed skin tissues of a 55-year-old female patient's left hand palmar fascia regions. The skin tissues were minced and enzymatically disaggregated using a 0.5% collagenase solution (250 U/mL Serva, Heidelberg, Germany)

at 37°C in 5% CO_2 for 6 hours. After centrifugation, the pellet was resuspended in culture medium (TC 199 with Earle salts supplemented with 20% fetal bovine serum, 200 IU/mL penicillin, 200 µg/mL streptomycin) and incubated at 37°C in 5% CO_2 air. The culture medium was changed after attachment of the cells. Primary fibroblasts of the 3 different skin tissues were passaged using trypsine/EDTA solution (0.05%/0.02% *w/v* in PBS w//o Ca^{2+}, Biochrom, Berlin, Germany) a split ratio of 1:2 one time a week to preserve monolayer formation. The patient had given informed consent. The study was approved by the local Ethics Committee (Ärztekammer Bremen, #336/2012). The guidelines of the declaration of Helsinki are followed.

All fibroblasts were cultured in DMEM medium and incubated at 37°C in a humidified atmosphere of 95% air and 5% CO_2. Medium was supplemented with 10% fetal bovine serum and 2% penicillin-streptomycin. Prior to cell seeding, PA gel substrates were sterilized in ethanol, extensively washed in PBS, and incubated with DMEM medium along with 20% fetal bovine serum for a few hours to promote serum protein adsorption on the gels, hence, cell adhesion (Rianna and Radmacher[22], see Figure S6). Cells were seeded 48 hours prior to AFM measurements, either plated on gels placed in Petri dishes or directly on Petri dishes. Passages between 3 and 7 were used for the experiments.

2.4 | AFM experiments

A MFP3D AFM (Asylum Research, Santa Barbara, California) was used to measure mechanical properties of 3 fibroblast types. Atomic force microscopy consists of 4 important components: (1) cantilevers with a pyramidal tip (in our case), (2) laser diode, (3) position sensitive photodetector, and (4) xyz piezoelectric scanner (Figure 1A). An optical microscope was combined with the AFM to be able to control tip and sample positioning. Soft cantilevers (MLCT Bio, Bruker, nominal spring constant 0.01 N/m) were used to investigate cell properties. The Petri dishes with cell samples were fixed to an aluminum holder with vacuum grease and mounted on the AFM stage with 2 magnets. The AFM head including the sample was enclosed in a homebuilt polymethacrylate (PMMA) box to inject and maintain 5% CO_2.

We used 2 cantilevers (same batch and same nominal spring constant) to minimize systematic errors due to calibration. The deflection sensitivity was adjusted offline based on the thermal tune and a spring constant of 10 mN/m as described in Schillers et al.[29]

2.5 | AFM force maps

Step response force curves were recorded on all 3 fibroblasts to study their viscoelastic properties. All force measurements were performed

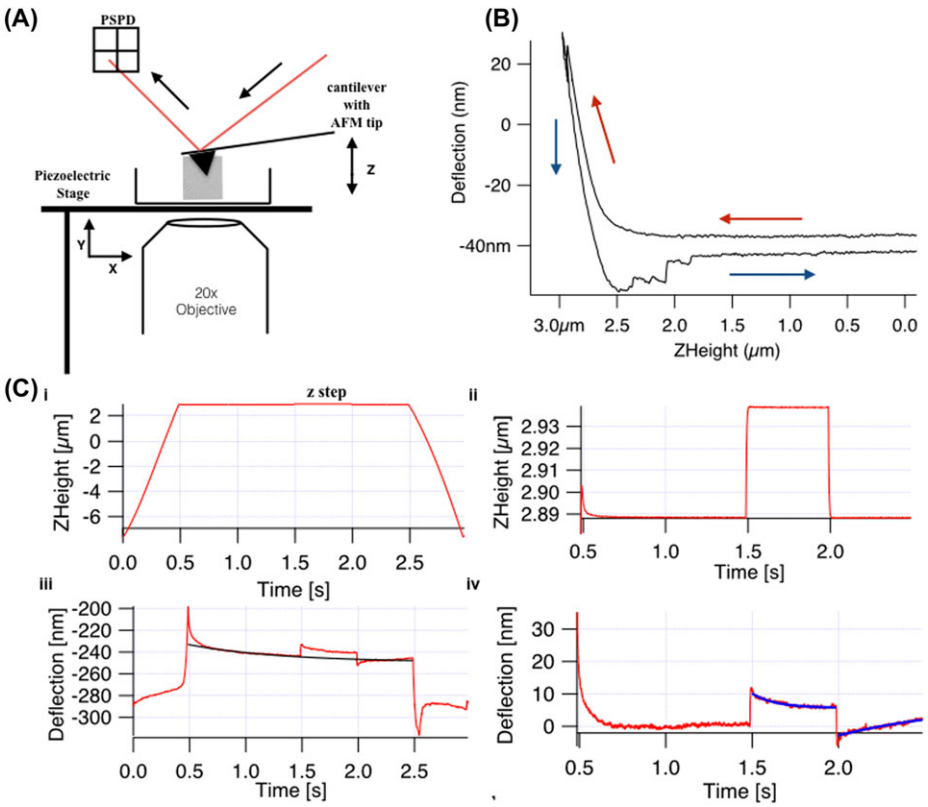

FIGURE 1 Basic components of (A) AFM and (B) force curve with (C) viscoelastic creep response measurement. A, The basic 4 components of AFM (i) a laser diode, (ii) a cantilever of 0.01 N/m spring constant with 30-nm radius AFM pyramidal tip, (iii) a position-sensitive photo detector (PSPD), and (iv) xyz-piezo stage. B, Sample indentation by the AFM tip obtains the force curve that gives the approach (red arrow) and retract (blue arrow) curve on deflection vs Z-height graph, and apparent Young modulus was calculated by applying Hertz model to the approach curve. In creep response curve (C), the Z-height profile (i) shows the approach and retract ramp towards the cell for 3 seconds, and in-between, there is a z step, which is applied at t = 1.5, which is enlarged in (ii). (iii) The deflection data show global creep of the cell, which includes the creep after loading and unloading step, which is enlarged in (iv), and global creep was determined by the exponential fit (black curve) and was subtracted for qualitative analysis

with 2 cantilevers. First, the spring constant of the cantilever was calibrated by using the thermal tune method,[30] and then force curves were recorded over different regions of cells (nuclear region, cell center, and periphery). For step response force curves, we used typically a scan rate of 1 Hz, corresponding to a maximum loading rate of 1 nN/s and a maximum force of 1 nN. Indentation depths were always greater than 500 nm to average the stiffness over a large contact area, which gives values that do not depend on local variations of the cytoskeleton structures. At least 25 cells were measured for each substrate; 256 force curves were acquired over a cell of scan size 30 μm called force maps. To apply the step, z motion was stopped for a dwell time of 2 seconds after the trigger threshold was achieved (cantilever deflection of 100 nm). After 1 second, the z height was changed by 50 nm towards the cell, and after an extra 0.5 seconds, this step was reversed.[26]

2.6 | AFM data analysis

The data analysis package IGOR (wave metrics, Lake Oswego, Oregon) was used to evaluate mechanical data of the cells. Details have been described elsewhere.[22] Recording force curves (Figure 1B), by approaching (red arrows) and retracting (blue arrows) the cantilever towards and from the sample, we obtained information on its mechanical properties. Force curves are usually analyzed within the framework of the Hertz model.[31-33] However, this model only considers the elastic response of the sample, neglecting the viscous response from certain samples (like cells), which is visible from a large hysteresis between approach (red arrows) and retract curves (blue arrows) (Figure 1B).

In step response curves, a well-defined z-step is applied while the tip is in contact with the sample (Figure 1C). After applying a loading force of 1 nN, the z-height was kept constant for 2 seconds to allow the cells to reach an equilibrium, and then a small step of 50 nm in z-height was applied at 1.5 seconds (Figure 1C). This small step is reversed after 0.5 seconds, the relaxation of the cell is observed, and after another 0.5 seconds, the tip is fully brought out of contact from the cell after a short time of period. Even though we waited for 1 second before applying the step to minimize creep caused by the approach ramp of the force curve, it was essential to subtract an exponential fit to remove residual creep. The individual exponential fits were applied to the data after the loading and unloading step. Each fit resulted in two spring constants and one value for the friction-damping coefficient. Step response data were collected and fitted with the standard linear solid model (Figure S1), which is a combination of 2 springs and a dashpot (also called a Zener model).[34] The spring constant k_1 correspond to the stiffness of the sample after relaxation. The sum of k_1 and k_2 corresponds to the initial stiffness of the sample after the step is applied, whereas the friction-damping f is responsible for the strain and stress relaxation. The spring constants and the friction damping coefficient can be converted to true elastic moduli and dynamic viscosity, respectively, assuming a Hertzian response of the sample taking in account the final loading force during the step. The equations and fit parameters used for creep response data and elastic modulus and dynamic viscosity calculation were presented in Supporting Information.

2.7 | Immunofluorescence staining

Forty-eight hours after seeding of cells on gels and Petri dishes, cells were fixed with 3.7% formaldehyde for 15 minutes and permeabilized with 0.1% Triton X100 for 3 minutes. Samples were washed with PBS after each step and then incubated with a rhodamine phalloidin solution (5:200 dilution in PBS) for F-actin staining for 30 minutes at 20°C . For α-SMA staining, cells were incubated with primary antibody anti-alpha-actin (smooth muscle) rabbit monoclonal antibody (1:100 dilution in 0.1% BSA/PBS) and followed by incubation with secondary antibody Alexa Fluor 488 (1:200 dilution in 0.1% BSA/PBS) for 30 minutes each at 20°C, and samples were washed after every step with 0.1% BSA/PBS. Finally, cells were stored in PBS at 4°C prior to image acquisition. An Axiovert 135 TV epifluorescence microscope (Carl Zeiss MicroImaging GmbH, Germany) with 40× objective lens was used to observe cells and collect fluorescent images.

2.8 | Wound healing assay

All 3 fibroblast types were seeded at a density of 2×10^5 on Petri dishes and incubated at 37°C in a 5% CO_2/air atmosphere until 100% confluence. Cell monolayers were scratched manually with a 10-μL pipette tip and then washed with PBS twice to remove cellular debris followed by replenishing with the fresh medium. To observe the migratory activity of the cells, we used a light microscopy (Axiovert 135, Carl Zeiss MicroImaging GmbH, Germany) with 20× objective lens. Images were recorded every 2 minutes for a total time of 24 hours. In the end, the scratch area before and after closure was calculated using Fiji software.[35] Specifically, we applied image thresholding and segmentation to separate our object of interest from the background (in this case the scratch area from the cell layer). Then, by using the macro *MRI Wound Healing Tool*,[22] we measured the area of the gap for each image and plot these data versus time. We used Manual Tracking Tool of Fiji software to monitor the velocity and trajectory of single cells at the scratch edge of the wound healing assay. More than 26 cells were tracked in each video, and totally 2 videos were studied for each cell types.

2.9 | Statistical analysis

Statistical differences for the median values of elastic moduli and dynamic viscosity of fibroblasts between different conditions of the AFM measurements were determined by Wilcoxon test, calculated in IGOR software. * and ** indicate statistically significant differences for P values < .05 and P < .005, respectively.

3 | RESULTS

The microenvironment of every cell is composed of chemical and physical components, which play a key role in influencing and determining cell fate and functions. Releasing specific components, cells modify the ECM, and vice versa, ECM influences cell processes in a dynamic interplay. To mimic certain properties of natural cellular environments, like mechanical properties, we provided cells with specific mechanical cues by using synthetic gels as cell culture supports.

Specifically, we prepared PA gels with 2 different stiffness values: soft (E, ~1 kPa) and stiff (E, ~50 kPa) gels. We measured the different stiffness values of the respective gels by AFM, recording force maps of 6 × 6 force curves within a 1-μm area on the gel surface. Force curves (Figure 2A,B) show the separation between approach and retract curves, which indicates that the viscosity is larger in stiff gels compared with soft gels. The difference between stiff and soft gels can be seen also in the graph showing force versus indentation in Figure S2. Moreover, with the step response experiment, the median values of apparent Young modulus and elastic modulus were obtained and listed in Table S1. The apparent Young modulus was calculated by using Hertz model on the approach curve of the force curve, which does not include the contribution of viscosity of the sample, whereas the elastic modulus was calculated from step response data by using the standard linear model, which also yields the dynamic viscosity of the sample. The difference in the apparent Young modulus and elastic modulus values is due to negligence of sample viscosity in the simple analysis using the Hertz model, whereas the standard linear model includes the viscous effect of the sample and thus gives the true elastic modulus value of the sample.

The mechanical properties of cells can often be related to their physiological or pathological state. In fact, cell mechanics has been previously used to discriminate between many healthy and diseased cells, like in the case of cancer, blood, and cardiovascular diseases.[21,23-25] In this study, we used AFM to study mechanical properties of normal, scar, and Dupuytren's fibroblasts (from the same patient) to investigate whether Dupuytren's fibroblasts could show a different mechanical phenotype compared with the other cell types. Moreover, we investigated the effect of TGF-β1 (5 ng/mL) on stress fiber formation in fibroblasts, hence in their stiffness. With this aim, we took 30-μm scan size force maps of 128 × 2 step response force curves over the nuclear, cell body and periphery region of a cell, and we could measure median values of elastic modulus of 2.1, 1.8, and 4.4 kPa for normal, scar, and Dupuytren's fibroblasts, respectively (Figure 3A, filled circles). Our results showed that Dupuytren's fibroblasts were much stiffer than the other 2 cell types, in both conditions, with and without TGF-β1 (Figure 3A, filled circles and triangles, respectively, and Figure S3A,B). Results are shown in Figure 3, and the respective values of the elastic modulus and the dynamic viscosity are listed in Tables 1 and 2. Moreover, we found that Dupuytren's fibroblasts increased their elastic modulus and becomes stiffer (Figure S3C) in presence of TGF-β1 (from 4.4 to 6.2 kPa), whereas we did not find significant changes in the elastic moduli of scar and normal fibroblasts, before and after addition of TGF-β1. To check whether cytoskeleton organization could have an influence on the mechanical properties of fibroblasts, we then acquired fluorescent images of the 3 cell types, staining α-SMA stress fibers. We found large differences in structure and organization of the cytoskeleton network in Dupuytren's fibroblasts compared with the other cells. In fact, Dupuytren's fibroblasts were characterized by a wide number of thick and well-organized stress fibers (Figure S4, left row), and bundles of stress fibers were even thicker in presence of TGF-β1 (Figure S4, right row). In normal and scar fibroblasts instead,

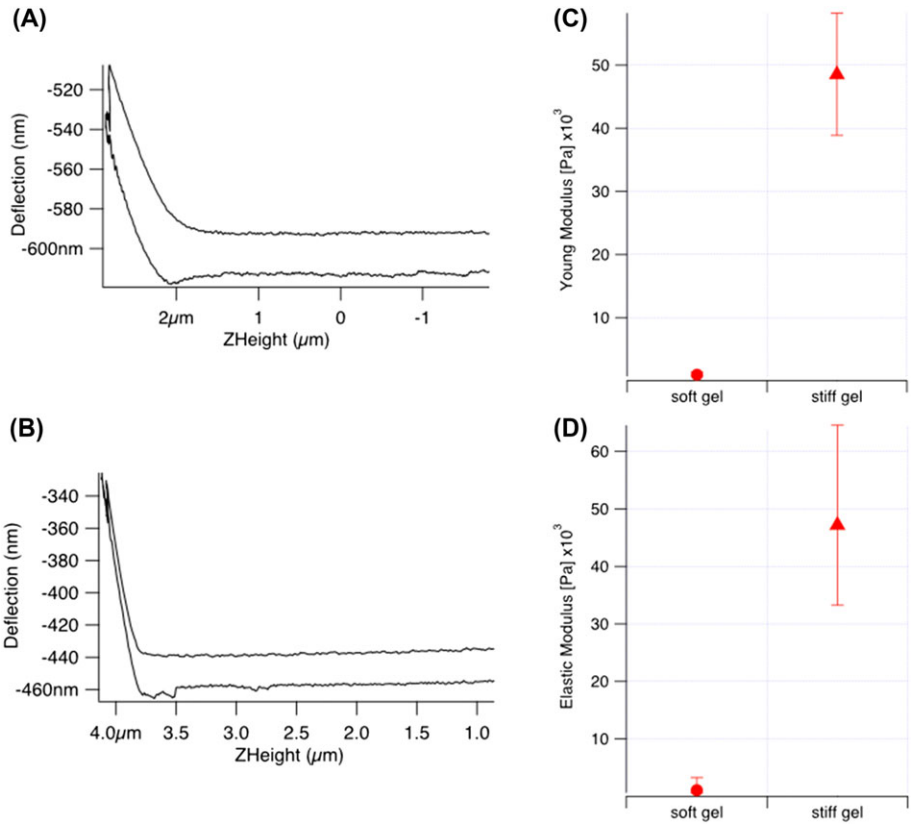

FIGURE 2 Force curve from (A) soft and (B) stiff gels and comparison of (C) apparent Young modulus and (D) elastic modulus. The force curves obtained on soft and stiff gels show the separation of approach and retract curves due to viscous contribution. This separation is larger in soft gel than in stiff gel force curve, thus resulting in changes in apparent Young modulus and elastic modulus values. The error bars of first and third quartiles are shown in Table S1

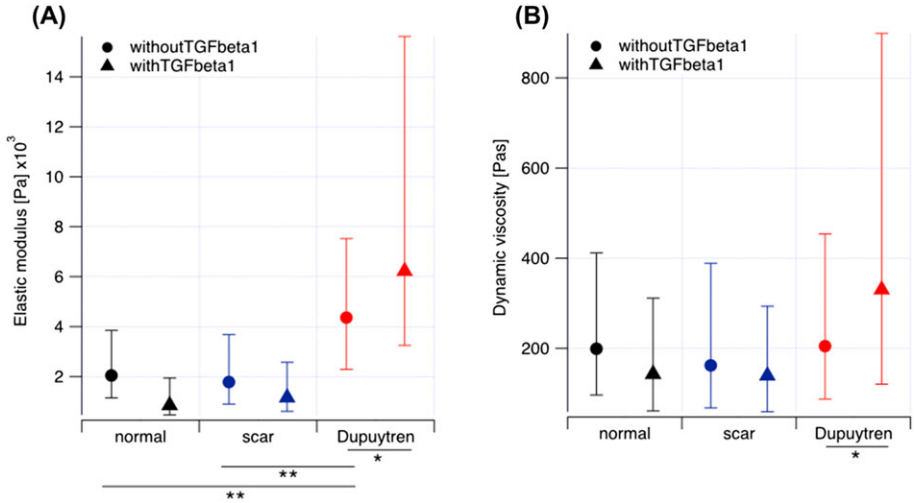

FIGURE 3 (A) Elastic modulus and (B) dynamic viscosity of fibroblasts with and without TGFβ1. The elastic modulus and dynamic viscosity graph for normal, scar, and Dupuytren's fibroblasts seeded on Petri dish in the presence (filled circle) and absence (filled triangle) of TGFβ1 clearly show that the Dupuytren's fibroblasts are stiffer and more viscous than the other fibroblasts in the presence of TGFβ1. For each category, maximum 29 number of cells were studied. The error bars of first and third quartiles are shown in Tables 1 and 2

TABLE 1 The median (bold values) elastic modulus values of normal, scar, and Dupuytren's fibroblasts treated with and without TGF-β1

Elastic Modulus, kPa	Without TGF-β1			With TGF-β1		
	25th	Median	75th	25th	Median	75th
Normal	0.8	**2**	1.8	0.3	**0.8**	1.0
Scar	0.8	**1.8**	1.9	0.3	**1.1**	1.4
Dupuytren's	2.1	**4.4**	3.2	2.9	**6.2**	9.3

TABLE 2 The median (bold values) dynamic viscosity values of normal, scar, and Dupuytren's fibroblasts treated with and without TGF-β1

Dynamic Viscosity, Pas	Without TGF-β1			With TGF-β1		
	25th	Median	75th	25th	Median	75th
Normal	102.8	**199**	212.9	81.7	**142.8**	168.6
Scar	94.3	**162.3**	226.7	79.8	**139.2**	154
Dupuytren's	117.8	**204.8**	248.8	209.8	**330.3**	568.3

cytoskeleton network did not undergo dramatic changes in presence of TGF-β1. Therefore, we found that variations in cytoskeleton structure, and specifically in α-SMA fibers number and conformation, could be related to an increase in elastic moduli in Dupuytren's fibroblasts. Additionally, we investigated the viscous properties of fibroblasts by performing step response force curves, and we found that Dupuytren's fibroblasts are also affected from TGF-β1 as they become more viscous (from 204 to 330 Pas) after application of TGF-β1 (Figure 3B). Therefore, from this first set of experiments, we could find that viscoelastic properties of Dupuytren's fibroblasts increase in presence of TGF-β1, while instead the other 2 types of fibroblasts are less affected. Moreover, we could associate the increase of Dupuytren's fibroblast stiffness to the presence of α-SMA stress fibers.

The relative stiffness of the matrix, which surrounds the cell, can have a strong influence on the biochemical (expression of biomolecules) and mechanical (stiffness) properties of the cell. To check whether mechanical properties of ECM could have an influence on the mechanical properties of the fibroblasts used in this study, we prepared different stiffness PA gels as cell substrates, and we used AFM to study the elastic and viscous response of normal, scar, and Dupuytren's fibroblasts seeded on them. Specifically, experiments were performed on cells seeded on PA gels with 2 different stiffness values (1 and 50 kPa) and on conventional Petri dishes as a control. Therefore, we took force maps with 128 × 2 force curves over the nuclear, cell body and periphery regions of 30-μm scan size (for cells on Petri dish and stiff gels) and 10-μm scan size (for cells on soft gels, since cells tended to be smaller and less spread on this substrate) and measured the elastic modulus and dynamic viscosity for the fibroblasts in the presence of TGF-β1. Results are shown in Figure 4, and the respective values of the elastic modulus and the dynamic viscosity are listed in Tables 3 and 4. We found a direct correlation between cell stiffness and substrate stiffness in Dupuytren's fibroblasts, ie, elastic moduli of fibroblasts decrease with decreasing stiffness of the underlying substrate. For the other 2 fibroblasts, we did not find this correlation. Moreover, to evaluate the stiffness, force versus indentation data were plotted for 3 fibroblasts (Figure S5A,B) on soft and stiff gels and specifically for Dupuytren's fibroblast (Figure S5C). We therefore confirmed that Dupuytren's fibroblasts were stiffer than other 2 fibroblasts and that they could adapt their stiffness to those of the underling gels. Fluorescent images presenting the expression of α-SMA stress fibers for different cell types on soft and stiff gels are reported in Figure S6, showing that all 3 fibroblast are more spread on stiff gel than on soft gel and they present α-SMA stress fibers on less compliant materials.

Cell migration plays an important role in wound healing. One of the most used assays to study cell migratory activity is the so-called wound healing or scratch assay. With this assay, a gap is mechanically created on a confluent layer of cells, and the migration of cell within the scratch is observed. We used this assay to gain information on cell velocity and motility. In our experimental setting, the migration of normal, scar, and Dupuytren's fibroblasts within the scratch area was monitored using light microscopy over an observation period of 24 hours

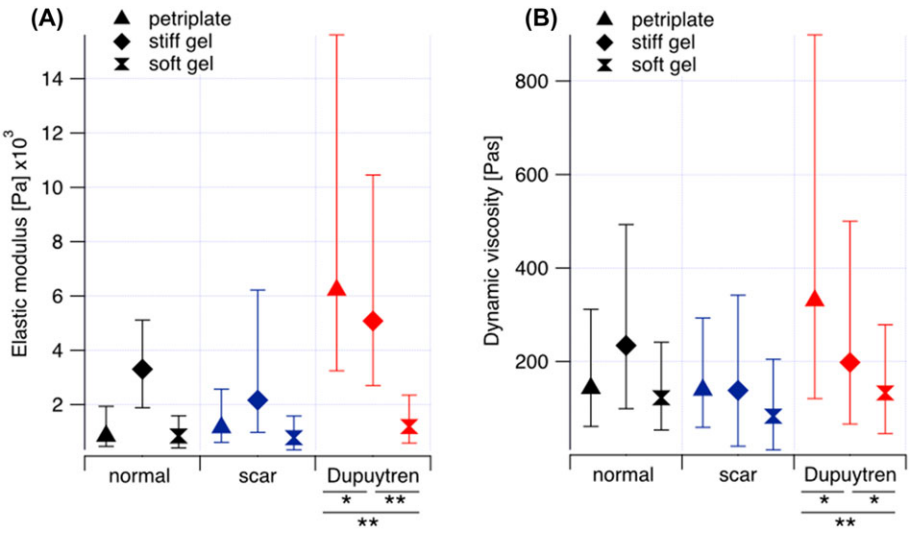

FIGURE 4 (A) Elastic modulus and (B) dynamic viscosity of fibroblasts on different stiffness substrates. The elastic modulus data for normal, scar, and Dupuytren's fibroblasts on a Petri dish (filled triangle), soft gel (filled rhombus), and stiff gel (filled double triangle) clearly show that the matrix stiffness that influences cell stiffness is most pronounced in Dupuytren's fibroblast, whereas in the others, it is rather negligible. The dynamic viscosity data for all fibroblasts show the differing viscous properties of normal, scar, and Dupuytren's fibroblasts on substrates. For each category, maximum 29 number of cells were studied. The error bars of first and third quartiles are shown in Tables 3 and 4

TABLE 3 The median (bold values) elastic modulus values of normal, scar, and Dupuytren's fibroblasts on Petri dish, soft gel, and stiff gel in the presence of TGF-β1

Elastic Modulus, kPa	Petri Dish			Soft Gel			Stiff Gel		
	25th	Median	75th	25th	Median	75th	25th	Median	75th
Normal	0.3	**0.8**	1.0	0.4	**0.8**	0.7	1.4	**3.3**	1.8
Scar	0.5	**1.1**	1.4	0.4	**0.7**	0.8	1.2	**2.2**	4.1
Dupuytren's	2.9	**6.2**	9.3	0.6	**1.2**	1.1	2.4	**5.1**	5.4

TABLE 4 The median (bold values) dynamic viscosity values of normal, scar, and Dupuytren's fibroblasts on Petri dish, soft gel, and stiff gel in the presence of TGF-β1

Dynamic Viscosity, Pas	Petri Dish			Soft Gel			Stiff Gel		
	25th	Median	75th	25th	Median	75th	25th	Median	75th
Normal	81.7	**142.8**	168.6	68.9	**122.5**	118.8	135.1	**234.4**	258.8
Scar	79.8	**139.2**	154	71.9	**83.2**	121.7	119.4	**138.1**	203.6
Dupuytren's	209.8	**330.3**	568.3	86.8	**132.9**	145.9	131.6	**198.2**	302

with images being taken every 2 minutes. In Figure S7, images are shown for 0 and 24 hours from left to right, respectively, taken from movies, which are provided in Movies S1, S2, and S3. The scratch area (~300 μm^2) was calculated by using ImageJ software for each frame from the 24-hour movie as described in Section 2. The scratch area (Figure 5A) was plotted against the time (each experiment was repeated twice) and found that α-SMA stress fibers expressing Dupuytren's fibroblasts could move at slower speed (Figure 5A, inset) within the scratch area compared with normal and scar fibroblasts. Moreover, from the single cell trajectories (Figure 5B), we could see that Dupuytren's fibroblasts cover a vertical distance (x axis) of ~50 μm within 24 hours. While instead, within the same range of time, scar and normal fibroblasts were able to cover longer distances (of ~100 μm). Thus, Dupuytren's fibroblast showed clear differences in their migratory properties compared with the other 2 fibroblasts.

4 | DISCUSSION

4.1 | Determining viscoelasticity by the standard linear solid model

The cytoskeletal filaments and the cytosol determine the elastic and viscous properties of cells. Most importantly, polymerization of monomer G-actin to filamentous F-actin affects the elastic properties of a cell. The concept of viscosity of a cell seems to be very complicated, eg, measured values depend on the length scale of the experiment, due to the complexity of the liquid, being a highly concentrated solution of molecules (proteins, RNA, oligosaccharides and the corresponding monomers, and ions and small organic molecules) and a mixture of larger structures like polymeric networks and organelles.[36] Elastic properties can be measured using magnetic twisting

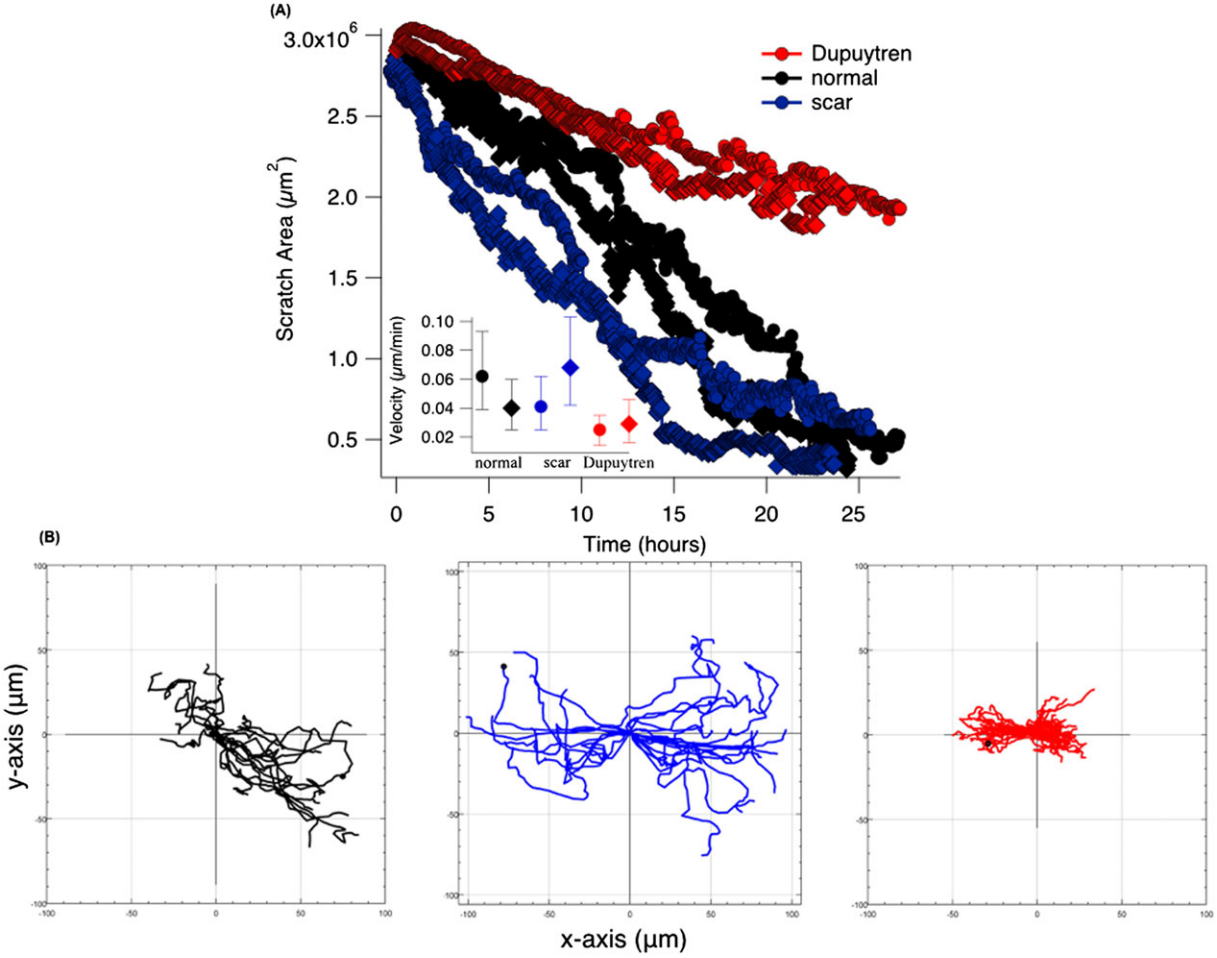

FIGURE 5 A, Scratch area as a function of time in the wound healing assay. For each cell type, we followed 2 samples over 24 to 28 hours. Closing of the gap was slowest for Dupuytren's cell (red trace) and faster for normal (black) and scar fibroblasts (blue). Closing of the gap correlates nicely with migration speed as calculating from tracks following individual cells in these experiments. The inset shows the median value of velocity values calculated by following individual cells from Movies S1 to S3. Dupuytren's fibroblast migrates at the speed of 0.026 μm/min, whereas normal and scar fibroblasts show migration speeds between 0.04 and 0.06 μm/s. B, Trajectories of normal (black), scar (blue), and Dupuytren's (red) fibroblasts were plotted by tracking individual cells from Movies S1, S2, and S3, respectively. Dupuytren's fibroblast migrates collectively, and thus, closure of the gap is much slower over the 24-hour time window

cytometry,[37] particle tracking,[38] and high-force magnetic tweezers[39] applying a force or torque on the cell. Viscous properties of cells can be measured by micropipette aspiration; however, this is restricted to nonadherent cells and will yield only one global value for the entire cell. Atomic force microscopy[40] gives us amble opportunities to determine the elastic properties of any area of interest in the cell by picking the appropriate tip geometry to choose a local measurement (eg, by using pyramidal tips) or a more extended global measurement by using spherical tips. In most cases, data are analyzed by using the Hertz model,[31,32] which neglects the effect of viscous properties. Thus, we should rather term the derived quantities apparent Young modulus. Here, by applying a small step of 50 nm during the contact with the cell and analyzing our step response data in the framework of standard linear solid model (Figure 3), we were able to determine the true elastic modulus and dynamic viscosity[26] (see Supporting Information for details). In this model, the sample is modeled by a Zener element with spring k_1 running parallel to Maxwell element consists of spring k_2 and a viscous damping coefficient f plus the cantilever spring of constant k_c in series. Z-height motion resulted in the deflection of the cantilever d, which can be fitted with the exponential function and indentation δ of the sample with the mathematic equation of $z = d + \delta$. We chose this very simple model[26] although there are many other models available for cell viscoelasticity like tensegrity model,[41] SGR model,[42] and poroelastic model,[43] since it is most appropriate to our experimental design, basically measuring only one relaxation time, ie, one mode of relaxation.

4.2 | PA hydrogels with regulated stiffness to mimic ECM

Mechanical properties of the ECM play a major role in cell development and morphogenesis.[44] The ECM microenvironment exerts physical stimuli, which result into mechanochemical and genetic alterations of cells. The mechanically compliant ECM provides cell adhesion and spreading by creation of cell focal adhesion points on ECM. Extracellular matrix microenvironment tackles the force created by cells, and this helps to study the mechanoresponse of cells on ECM substrate. The ECM consists of collagen, proteoglycans, fibrin, glycoproteins

and glycosaminoglycans (GAG), and other proteins. In some experimental settings, cells are studied on collagen hydrogels or collagen-GAG artificial matrixes, but tuning the stiffness of these gels to values close to those in tissues and presenting the cells adequately for AFM (ie, well adherent on the surface of the gel) turned out to be difficult. Thus, we choose to use here nonphysiological, but bio-inert PA gels. The stiffness of thin PA hydrogels can be easily modulated by tuning the concentration of monomer and cross-linker, namely, acrylamide and bisacrylamide.[45] Here, we chose 2 values for the stiffness, ie, soft gels around 1 kPa that resemble the stiffness of most tissues (50 Pa-12 kPa)[46] and a stiffer value of 50 kPa that is considered as very stiff regarding cellular properties even though this value is much softer than conventional cell culture substrates, such as Petri dishes.

4.3 | Dupuytren's fibroblasts are stiffer than normal or scar fibroblasts

By using AFM step response curves, we observed that pathological Dupuytren's fibroblasts are stiffer than other 2 types of fibroblasts, presumably due to the presence of α-SMA expression in intracellular stress bundles. This shows that the Dupuytren's fibroblasts are present in myofibroblast phenotype. In our experimental setting, the addition of 5 ng/mL TGF-β1 increased the expression of α-SMA and thus the elastic modulus predominantly in Dupuytren's fibroblasts, which further confirms their myofibroblast phenotype, whereas there is no significant response from normal and scar fibroblast to TGF-β1. Obviously, palmar fascial fibroblasts from Dupuytren's nodules and cords seem to react more rapidly to the TGF-β1 stimulus by expressing morphological and biochemical characteristics of smooth muscle cells.[47] The prominent biochemical α-SMA expression of vascular smooth muscle is also seen in fibroblasts from Dupuytren's environment other than β- and γ-cytoplasmic actins. These specialized fibroblasts that express α-SMA, exert high contractile force on ECM and synthesis, and remodel ECM are called myofibroblast. α-SMA is a cell-specific actin isoform, and its intracellular gene expression is activated by extracellular latent TGF-β1, which gets activated either by myofibroblast-derived ECM stretching[7] or autocrine production.[48]

The cell mechanics of myofibroblasts is not thoroughly investigated yet. Our results from step response measurements support the assumption that the expression of α-SMA in Dupuytren's fibroblasts is associated with increased stiffness and viscosity compared with normal and scar fibroblasts. After addition of TGF-β1, the stiffness of Dupuytren's fibroblasts increased further. Although previous studies[8,11] reported on the role of TGF-β1 on α-SMA expression and myofibroblast differentiation, there are no reports on the comparison of mechanical measurement of fibroblasts of different origins, mostly from normal and diseased tissues. Here, we measured cellular viscoelasticity, which reveals the different levels of intracellular force generation from each fibroblast type and their phenotype varied regarding α-SMA expression. Even when seeded on an "infinite" stiff substrate, as a Petri dish occurs to cells, normal fibroblasts and scar fibroblasts do not show a myofibroblast phenotype. This seems to be related to their different cytoskeleton organization, as we found a lack of stress fiber formation although they show low level α-SMA expression (Figure S4).

4.4 | Substrate stiffness influences the stiffness of Dupuytren's fibroblasts

Mechanical stress regulates myofibroblast differentiation and function. Fibroblasts are influenced by cell-ECM interactions, where they will, for instance, undergo stress-dependent maturation and form focal adhesion. The mechanical stress of the ECM is transmitted through the integrin-focal adhesion protein complex, which activates downstream signaling cascades in the cell resulting in the recruitment of α-SMA into stress fibers. Matrix stiffness plays a pivotal role in the fibroblast to myofibroblast transition.[49,50] In our study, we clearly observed the adaptive nature of Dupuytren's fibroblasts stiffness to matrix stiffness, which was less prominent with the other 2 types of fibroblasts in the current experimental setting. Dupuytren's fibroblasts were well adherent and well spread on Petri dishes as compared with normal fibroblasts and scar fibroblasts cells. As a consequence, they showed a larger cell area. In soft gels, all 3 types of fibroblasts are reduced in area and exhibit a more roundish shape. Generally, soft substrates led to the formation of less stress fibers, resulting in low values of elastic moduli for all 3 fibroblasts. Previous studies[51] showed that the focal adhesion area and α-SMA localization depends on matrix compliance. This explains that through focal adhesion (FA) points, Dupuytren's fibroblasts make stronger cell-ECM contacts on Petri dish and stiff gel (immunofluorescence data not performed), where α-SMA is recruited into stress fibers and becomes stiffer on both substrate. Even though normal and scar fibroblasts stiffness was influenced by PA substrate stiffness, they were soft even on a virtually incompressible stiff substrate (Petri dish) as they did not form more stress fibers even in the presence of TGF-β1. In the previous studies,[27] it was reported that NIH-3T3 fibroblasts show adaptive increasing cell size and stiffness with increasing gel stiffness coated with fibronectin. This could be due to the presence of fibronectin, which brings stronger adhesion, hence cell stiffness, and also due to fibroblast line from mice that attained different morphology and function than the cells used here. We used fibroblasts from human origin cultured on soft and stiff gels that enable good adhesion to the PA hydrogel. Recently, it was reported[52] that human dermal fibroblast cultured in 3D collagen matrix needed 3 weeks to form stress fibers and, with TGF-β1 presence, this still required 1 week. But in our study, prior to viscoelastic measurement within 48 hours of growth for all 3 cells in the presence and absence of TGF-β1, Dupuytren's fibroblasts are stiffer than the other 2 types of fibroblasts due to the myofibroblast phenotype. To prove the statement on myofibroblast differentiation, all 3 fibroblasts were grown for a week with TGF-β1 treatment. Differentiated myofibroblasts showed an increase in elastic moduli in all 3 cell types (Figure S8 and Table S2).

4.5 | Dupuytren's fibroblast migration

Here, we studied the wound healing assay for fibroblasts of 3 different origins and observed the difference in their migration pattern to close a mechanically created "wound gap." From Figure 5 and Movies S1, S2, and S3, it can be clearly seen that the Dupuytren's fibroblasts migrate slowly compared with the other ones, which might be due to their phenotypic presence of expressing α-SMA stress fibers.

Previously, it was discussed that filamentous α-SMA stress fibers expression immobilized the cells by forming prominent focal adhesion and thus reduced their motility.[53] Dupuytren's fibroblasts, which exhibit the myofibroblast phenotype, tend to move collectively to close the gap. The distance traveling within 24 hours is smaller than 50 μm. These myofibroblasts are the mechanically active cells that communicate through intercellular adherent junctions[54] and are also participating in the fibrosis in vivo.[55] Thus, exhibiting stronger cell-cell contact, Dupuytren's fibroblast from the fibrosis microenvironment migrates slowly in the scratch area. Scar fibroblasts are basically extracted from the wounded region. Apparently, they can sense the free space, enabling them to migrate and close the scratch faster than Dupuytren's cells. Recently,[56] a cell motility assay on skin fibroblasts from wild type and transgenic mice overexpressing PEA-15 protein showed that the wild-type cells sensed and closed the scratch faster than transgenic mice. Here, normal fibroblasts migrate individually in the same way as scar fibroblasts. In comparing the individual cell trajectories, scar fibroblast motility is more directed than the motility of normal fibroblasts, whereas Dupuytren's fibroblasts move in a "zig-zag" manner within the cell layer and thus were not able to achieve closing the gap within the observation period of 24 hours.

5 | CONCLUSIONS

We measured the viscoelastic properties of 3 types of fibroblast extracted from different tissues of the same patient: normal, scar, and Dupuytren's fibroblasts. We investigated the effect of TGF-β1 and microenvironment stiffness on fibroblast mechanical properties and cytoskeleton organization. We used different stiffness PA gels as cell culture substrates to reproduce an environment similar to the natural ECM (from the mechanical point of view) to study cell response to different mechanical signals. We could find differences in the way normal and diseased cells perceive and react to these external factors. Specifically, we found that Dupuytren's fibroblasts were stiffer and more viscous than normal- and scar-derived fibroblasts. Also, a pronounced relation between cell and matrix stiffness was found only for Dupuytren's fibroblasts, ie, the stiffness of these fibroblasts increased increasing the stiffness of the underling gels. Finally, from a wound healing assay, we found differences in the way different fibroblasts migrate, in terms of migration pattern and migration velocity: Dupuytren's fibroblasts migrated slowly, thus covering only shorter distances. Our findings show that the use of biophysical tools to investigate mechanical and migratory properties can help to discriminate between different cell phenotypes, highlighting differences between the way normal and diseased cells interact with their ECM and adapt their features.

AUTHOR CONTRIBUTIONS

P.K. performed AFM experiments, data analysis, and manuscript preparation. C.R. prepared gels and was involved in data analysis and manuscript preparation. G.B. established cell lines from primary cells. UM designed the experimental scheme. M.R. designed the experimental scheme and was involved in data acquisition, data analysis, and preparation of the manuscript.

ACKNOWLEDGEMENTS

We thank Holger Doschke for developing the data acquisition and analysis software and also for helpful discussions. AFM probes were a kind gift of Bruker, Santa Barbara, California.

CONFLICT OF INTEREST

The authors declare no conflicts of interest.

ORCID

Manfred Radmacher http://orcid.org/0000-0001-8744-4541

REFERENCES

1. van Beuge MM, ten Dam EJ, Werker PM, Bank RA. Matrix and cell phenotype differences in Dupuytren's disease. *Fibrogenesis Tissue Repair*. 2016;9(1):9.
2. Schleip R, Klingler W, Lehmann-Horn F. Fascia is able to contract in a smooth muscle-like manner and thereby influence musculoskeletal mechanics. *J Biomech*. 2006;39:S488.
3. Brickley-Parsons DI, Glimcher MJ, Smith RJ, Albin R, Adams JP. Biochemical changes in the collagen of the palmar fascia in patients with Dupuytren's disease. *JBJS*. 1981;63(5):787-797.
4. Rudolph R, Vande BJ. The myofibroblast in Dupuytren's contracture. *Hand Clin*. 1991;7(4):683-692.
5. Jemec B, Linge C, Grobbelaar AO, Smith PJ, Sanders R, McGrouther DA. The effect of 5-fluorouracil on Dupuytren's fibroblast proliferation and differentiation. *Chir Main*. 2000;19(1):15-22.
6. Kloen P, Jennings CL, Gebhardt MC, Springfield DS, Mankin HJ. Transforming growth factor-β: possible roles in Dupuytren's contracture. *J Hand Surg*. 1995;20(1):101-108.
7. Wipff PJ, Rifkin DB, Meister JJ, Hinz B. Myofibroblast contraction activates latent TGF-β1 from the extracellular matrix. *J Cell Biol*. 2007;179(6):1311-1323.
8. Desmoulière A, Geinoz A, Gabbiani F, Gabbiani G. Transforming growth factor-beta 1 induces alpha-smooth muscle actin expression in granulation tissue myofibroblasts and in quiescent and growing cultured fibroblasts. *J Cell Biol*. 1993;122(1):103-111.
9. Serini G, Bochaton-Piallat ML, Ropraz P, et al. The fibronectin domain ED-A is crucial for myofibroblastic phenotype induction by transforming growth factor-β1. *J Cell Biol*. 1998;142(3):873-881.
10. Tomasek JJ, Gabbiani G, Hinz B, Chaponnier C, Brown RA. Myofibroblasts and mechano-regulation of connective tissue remodelling. *Nat Rev Mol Cell Biol*. 2002;3(5):349-363.
11. Orlandi A, Ropraz P, Gabbiani G. Proliferative activity and α-smooth muscle actin expression in cultured rat aortic smooth muscle cells are differently modulated by transforming growth factor-β1 and heparin. *Exp Cell Res*. 1994;214(2):528-536.
12. Radmacher M. Measuring the elastic properties of biological samples with the AFM. *IEEE Eng Med Biol Mag*. 1997;16(2):47-57.
13. Radmacher M, Fritz M, Kacher CM, Cleveland JP, Hansma PK. Measuring the viscoelastic properties of human platelets with the atomic force microscope. *Biophys J*. 1996;70(1):556-567.
14. Friedrichs J, Torkko JM, Helenius J, et al. Contributions of galectin-3 and-9 to epithelial cell adhesion analyzed by single cell force spectroscopy. *J Biol Chem*. 2007;282(40):29375-29383.
15. Lehenkari PP, Horton MA. Single integrin molecule adhesion forces in intact cells measured by atomic force microscopy. *Biochem Biophys Res Commun*. 1999;259(3):645-650.
16. Beckmann J, Schubert R, Chiquet-Ehrismann R, Müller DJ. Deciphering teneurin domains that facilitate cellular recognition, cell-cell adhesion, and neurite outgrowth using atomic force microscopy-based single-cell force spectroscopy. *Nano Lett*. 2013;13(6):2937-2946.

17. Taubenberger AV, Hutmacher DW, Muller DJ. Single-cell force spectroscopy, an emerging tool to quantify cell adhesion to biomaterials. *Tissue Eng Part B Rev*. 2013;20(1):40-55.
18. Friedrichs J, Werner C, Müller DJ. Quantifying cellular adhesion to covalently immobilized extracellular matrix proteins by single-cell force spectroscopy. *Adhesion Protein Protocols*. 2013;19-37.
19. Kole TP, Tseng Y, Jiang I, Katz JL, Wirtz D. Intracellular mechanics of migrating fibroblasts. *Mol Biol Cell*. 2005;16(1):328-338.
20. Rotsch C, Radmacher M. Drug-induced changes of cytoskeletal structure and mechanics in fibroblasts: an atomic force microscopy study. *Biophys J*. 2000;78(1):520-535.
21. Rianna C, Radmacher M. Cell mechanics as a marker for diseases: biomedical applications of AFM. InAIP Conference Proceedings 2016 Aug 2 (Vol. 1760, no. 1, p. 020057). AIP Publishing
22. Rianna C, Radmacher M. Comparison of viscoelastic properties of cancer and normal thyroid cells on different stiffness substrates. *Eur Biophys J*. 2017;46(4):309-324.
23. Guedes AF, Carvalho FA, Malho I, Lousada N, Sargento L, Santos NC. Atomic force microscopy as a tool to evaluate the risk of cardiovascular diseases in patients. *Nat Nanotechnol*. 2016;11(8):687.
24. Stolz M, Gottardi R, Raiteri R, et al. Early detection of aging cartilage and osteoarthritis in mice and patient samples using atomic force microscopy. *Nat Nanotechnol*. 2009;4(3):186.
25. Dulińska I, Targosz M, Strojny W, et al. Stiffness of normal and pathological erythrocytes studied by means of atomic force microscopy. *J Biochem Biophys Methods*. 2006;66(1–3):1-1.
26. Yango A, Schäpe J, Rianna C, Doschke H, Radmacher M. Measuring the viscoelastic creep of soft samples by step response AFM. *Soft Matter*. 2016;12(40):8297-8306.
27. Solon J, Levental I, Sengupta K, Georges PC, Janmey PA. Fibroblast adaptation and stiffness matching to soft elastic substrates. *Biophys J*. 2007;93(12):4453-4461.
28. Tse JR, Engler AJ. Preparation of hydrogel substrates with tunable mechanical properties. *Curr Protoc Cell BiolCurrent protocols in cell biology*. 2010;10-16.
29. Schillers H, Rianna C, Schäpe J, et al. Standardized nanomechanical atomic force microscopy procedure (SNAP) for measuring soft and biological samples. *Sci Rep*. 2017;7(1):5117.
30. Sader JE, Larson I, Mulvaney P, White LR. Method for the calibration of atomic force microscope cantilevers. *Rev Sci Instrum*. 1995;66(7):3789-3798.
31. Hertz H. Über die Berührung fester elastischer Körper. *J für Die Reine Und Angewandte Mathematik*. 1882;92:156-171.
32. Sneddon IN. The relation between load and penetration in the axisymmetric Boussinesq problem for a punch of arbitrary profile. *Int J Eng Sci*. 1965;3(1):47-57.
33. Rico F, Roca-Cusachs P, Gavara N, Farré R, Rotger M, Navajas D. Probing mechanical properties of living cells by atomic force microscopy with blunted pyramidal cantilever tips. *Phys Rev E*. 2005;72(2):021914.
34. Fung YC. Biomechanics ASME. *Appl Mech Rev*. 1985;38(10):1251-1255.
35. Schindelin J, Arganda-Carreras I, Frise E, et al. Fiji: an open-source platform for biological-image analysis. *Nat Methods*. 2012;9(7):676-682.
36. Kalwarczyk T, Ziebacz N, Bielejewska A, et al. Comparative analysis of viscosity of complex liquids and cytoplasm of mammalian cells at the nanoscale. *Nano Lett*. 2011;11(5):2157-2163.
37. Coughlin MF, Fredberg JJ. Changes in cytoskeletal dynamics and nonlinear rheology with metastatic ability in cancer cell lines. *Phys Biol*. 2013;10(6):065001.
38. Gal N, Weihs D. Intracellular mechanics and activity of breast cancer cells correlate with metastatic potential. *Cell Biochem Biophys*. 2012;63(3):199-209.
39. Kollmannsberger P, Fabry B. BaHigh-force magnetic tweezers with force feedback for biological applications. *Rev Sci Instrum*. 2007;78(11):114301.
40. Binnig G, Quate CF, Gerber C. Atomic force microscope. *Phys Rev Lett*. 1986;56(9):930.
41. Ingber DE. Tensegrity: the architectural basis of cellular mechanotransduction. *Annu Rev Physiol*. 1997;59(1):575-599.
42. Sollich P. Rheological constitutive equation for a model of soft glassy materials. *Phys Rev E*. 1998;58(1):738.
43. Moeendarbary E, Valon L, Fritzsche M, et al. The cytoplasm of living cells behaves as a poroelastic material. *Nat Mater*. 2013;12(3):253-261.
44. Enemchukwu NO, Cruz-Acuña R, Bongiorno T, et al. Synthetic matrices reveal contributions of ECM biophysical and biochemical properties to epithelial morphogenesis. *J Cell Biol*. 2015. jcb-201506055
45. Denisin AK, Pruitt BL. Tuning the range of polyacrylamide gel stiffness for mechanobiology applications. *ACS Appl Mater Interfaces*. 2016;8(34):21893-21902.
46. Cox TR, Erler JT. Remodeling and homeostasis of the extracellular matrix: implications for fibrotic diseases and cancer. *Dis Model Mech*. 2011;4(2):165-178.
47. Tomasek J, Rayan GM. Correlation of α-smooth muscle actin expression and contraction in Dupuytren's disease fibroblasts. *J Hand Surg*. 1995;20(3):450-455.
48. Dabiri G, Campaner A, Morgan JR, Van De Water L. A TGF-β1-dependent autocrine loop regulates the structure of focal adhesions in hypertrophic scar fibroblasts. *J Invest Dermatol*. 2006;126(5):963-970.
49. Li Z, Dranoff JA, Chan EP, Uemura M, Sévigny J, Wells RG. Transforming growth factor-β and substrate stiffness regulate portal fibroblast activation in culture. *Hepatology*. 2007;46(4):1246-1256.
50. Smithmyer ME, Sawicki LA, Kloxin AM. Hydrogel scaffolds as in vitro models to study fibroblast activation in wound healing and disease. *Biomater Sci*. 2014;2(5):634-650.
51. Goffin JM, Pittet P, Csucs G, Lussi JW, Meister JJ, Hinz B. Focal adhesion size controls tension-dependent recruitment of α-smooth muscle actin to stress fibers. *J Cell Biol*. 2006;172(2):259-268.
52. Achterberg VF, Buscemi L, Diekmann H, et al. The nano-scale mechanical properties of the extracellular matrix regulate dermal fibroblast function. *J Investig Dermatol*. 2014;134(7):1862-1872.
53. Rønnov-Jessen L, Petersen OW. A function for filamentous alpha-smooth muscle actin: retardation of motility in fibroblasts. *J Cell Biol*. 1996;134(1):67-80.
54. Follonier L, Schaub S, Meister JJ, Hinz B. Myofibroblast communication is controlled by intercellular mechanical coupling. *J Cell Sci*. 2008;121(20):3305-3316.
55. Bochaton-Piallat ML, Gabbiani G, Hinz B. The myofibroblast in wound healing and fibrosis: answered and unanswered questions. F1000Research 2016;5.
56. Ascione F, Vasaturo A, Caserta S, D'Esposito V, Formisano P, Guido S. Comparison between fibroblast wound healing and cell random migration assays in vitro. *Exp Cell Res*. 2016;347(1):123-132.

SUPPORTING INFORMATION

Additional Supporting Information may be found online in the supporting information tab for this article.

How to cite this article: Viji Babu PK, Rianna C, Belge G, Mirastschijski U, Radmacher M. Mechanical and migratory properties of normal, scar, and Dupuytren's fibroblasts. *J Mol Recognit*. 2018;e2719. https://doi.org/10.1002/jmr.2719